

Variable Speed Optimization of a Vibro-impact Capsule System in Both the Forward and Backward Directions



Yang Zheng, Maolin Liao, Jiajia Zhang, Yang Liu, Jiapeng Zhu, and Zhiqiang Zhu

1 Introduction

The wireless capsule endoscopy detection technology was proposed about 20 years ago [1]. Due to its significant advantages on being painless, noninvasive, and free of anesthesia and having no cross infection, the wireless capsule endoscopy thoroughly changed the traditional endoscopy detection by using wired endoscopy. At present, the capsule endoscope for clinical application either moves passively depending on gastrointestinal motility or is controlled by an external magnetic field [2, 3]; thus, the capsule does not own the independent capacity of movement. Under such circumstances, the research about the self-propulsion capsule has gradually become a hotspot. Liu et al. proposed a model about the vibro-impact capsule system [4–6] and conducted a series of experimental studies to demonstrate the numerical results obtained according to their dynamic model [7–9]. Based on their work, the further consideration is how to effectively control the movement direction and speed of the self-propulsion capsule, which will be discussed in this paper.

Y. Zheng · M. Liao (✉) · J. Zhu · Z. Zhu

School of Mechanical Engineering, University of Science and Technology Beijing, Beijing, China
e-mail: liaomaolin@ustb.edu.cn

J. Zhang · Y. Liu

College of Engineering, Mathematics, and Physical Sciences, University of Exeter, Exeter, UK

2 Mathematical Modelling

In this section, a mathematical model about the vibro-impact self-propulsion capsule system is introduced. The physical model is simplified from the actual capsule, based on which the dynamic model is developed.

2.1 Physical Model

The physical model of a vibro-impact self-propulsion capsule is shown in Fig. 1, where M_c and M_m are the masses of the capsule and the magnet, respectively. k_1 and c represent the stiffness of the helical spring connecting the magnet and the capsule and the damping coefficient of the energy dissipation led by the relative speed between the capsule and the magnet, respectively. The springs with stiffness k_2 and k_3 represent the primary and the secondary constraints, and their gaps between the magnet and the constraints are G_2 and G_3 , respectively. A pre-compressed distance of the physical spring is defined as G_1 . X_c and X_m are the displacements of the capsule and the magnet, and their velocities are V_c and V_m , respectively. In addition, F_f , F_e , and F_i are the external frictional force, the inner excitation force, and the impact force between the capsule and the magnet, respectively. All the structure parameters for the capsule system are listed in Table 1.

2.2 Dynamic Model

Based on the physical model shown in Fig. 1, the corresponding mathematical model can be developed as [10].

$$\begin{cases} M_m \ddot{X}_m = F_i \\ M_c \ddot{X}_c = F_f - F_i \end{cases} \quad (1)$$

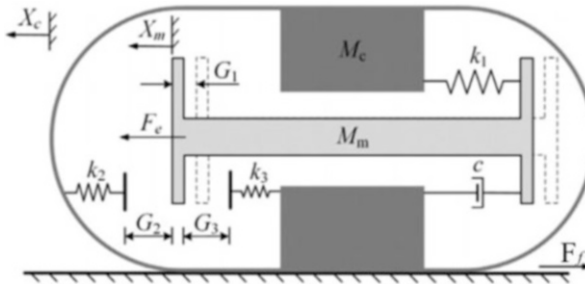


Fig. 1 Physical model of a vibro-impact self-propulsion capsule [10]

Table 1 Structure parameters of the capsule system

Parameters	Unit	Values
M_c	g	1.8
M_m	g	1.67
G_1	mm	0
G_2	mm	1.6
G_3	mm	0
k_1	kN/m	0.062
k_2	kN/m	27.9
k_3	kN/m	53.5
c	Ns/m	0.0156

where

$$F_f = \begin{cases} -\text{sign}(V_c) \cdot \mu (M_m + M_c) \text{ g}, & V_c \neq 0 \\ \text{sign}(F_i) \cdot \mu (M_m + M_c) \text{ g}, & V_c = 0, |F_i| \geq \mu (M_m + M_c) \text{ g} \\ F_i, & V_c = 0, |F_i| \leq \mu (M_m + M_c) \text{ g} \end{cases} \quad (2)$$

$$F_i = \begin{cases} F_e - F_1 - c(V_m - V_c) - F_3, & X_m - X_c \leq -G_3 \\ F_e - F_1 - c(V_m - V_c), & -G_3 \leq X_m - X_c \leq G_2 \\ F_e - F_1 - c(V_m - V_c) - F_2, & X_m - X_c \geq G_2 \end{cases} \quad (3)$$

$$F_e(t) = \begin{cases} P_d, & t \in \left[n \frac{1}{f}, n \frac{1}{f} + D \frac{1}{f} \right] \\ 0, & t \in \left(n \frac{1}{f} + D \frac{1}{f}, n \frac{1}{f} + \frac{1}{f} \right) \end{cases} \quad (4)$$

$$\begin{cases} F_1 = k_1 (X_m - X_c + G_1) \\ F_2 = k_2 (X_m - X_c - G_2) \\ F_3 = k_3 (X_m - X_c + G_3) \end{cases} \quad (5)$$

where n is the period number and P_d , f , and D are the amplitude, frequency, and duty cycle ratio of the excitation signal, respectively. Moreover, in order to compare the variable speed of the vibro-impact capsule, its average velocity is calculated as follows:

$$v_{\text{avg}} = \frac{f}{n} \left(X_c \left(n \frac{1}{f} \right) - X_c(0) \right) \quad (6)$$

3 Optimization Design

The precise control of both the speed and the direction for the capsule movement in uncertain small-bowel circumstance is a challenging task. For such a purpose, to better describe the dynamic responses of the capsule, seven variable speed steps are proposed, including fast backward and forward movements, medium-speed backward and forward movements, slow backward and forward movements, and hover movement under gastrointestinal motility. In addition, for a given capsule system, the excitation signal is convenient to be adjusted; hence, the optimization parameters consist of the frequency (f), amplitude (P_d), and duty cycle ratio (D) of the excitation square signal. Moreover, the uncertainty of the friction coefficient (μ) due to the varied structure and lubrication of the practical small bowel is also considered as an environment variable. The purpose of optimization is to find the best combination of parameters within the respective ranges of the given parameters to make the capsule move with the speed closest to the proposed speed step. To conduct the speed optimization, the dynamic model built in MATLAB is introduced into Isight, since Isight integrates a group of optimization algorithms which can be redesigned and combined to complete an optimization task with high efficiency and high accuracy.

3.1 Optimization Algorithms and Flow Path

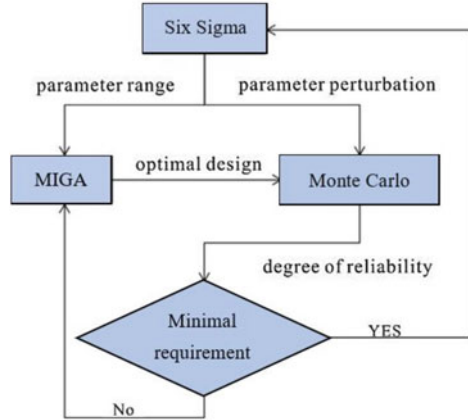
As aforementioned, there are three optimization parameters, one environment variable, and one optimization objective; hence, this is a multiparameter and single-objective optimization. Furthermore, in order to secure the reliability of the obtained optimization solutions in uncertain practical small-bowel environmental, parameter perturbations should be considered accompanying with the optimization. Therefore, a combination of the optimization algorithms is considered. Specifically, Multi-Island Genetic Algorithm (MIGA) is chosen to conduct the optimization, while Monte Carlo algorithm is applied in measuring the degrees of reliability of the optimal solutions provided by MIGA. Moreover, both the MIGA and the Monte Carlo method are driven by the Six Sigma algorithm which secures that all the confirmed optimal solutions satisfy a predefined minimal degree of reliability, which is set as 99% in this present work, and finally, the steady optimization designs can thus be extracted from massive parameter combinations. The flow path of this combined optimization is illustrated in Fig. 2.

The detailed optimization model for this combined optimization algorithms can be introduced as follows:

$$X_L + \Delta X \leq X \leq X_U - \Delta X \quad (7)$$

$$Z_L \leq Z \leq Z_U \quad (8)$$

Fig. 2 Flow chart of the combined optimization algorithms



$$\text{Lower limit} \leq G = \mu_Y(X, Z) + n\sigma_Y(X, Z) \leq \text{Upper limit} \tag{9}$$

$$\text{Minimize } F(\mu_Y(X, Z), \sigma_Y(X, Z)) = \left[(\mu_Y(X, Z) - M)^2 - \sigma_Y(X, Z)^2 \right] \tag{10}$$

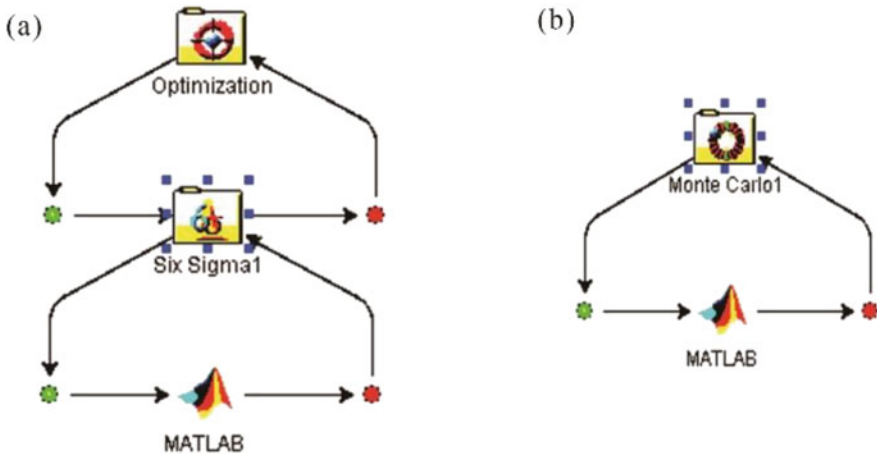
where X represents the design variables, including the frequency, amplitude, and duty cycle ratio of the excitation square signal, and X_L , X_U , and $\pm\Delta X$ are the lower and upper limits and the fluctuation range for the design parameters, respectively. Z represents the environmental variable, namely, the uncertainty of the friction coefficient in the small bowel; Z_L and Z_U are its lower and upper limits. G is the constraint condition, where the accepted velocity range for the capsule movement in each optimization case can be set. $\mu_Y(X, Z)$ and $\sigma_Y(X, Z)$ represent the average velocity of the capsule and its standard deviation, respectively. n is the number of sigma; when $n = 6$, the reliability of the optimization result is the highest; hence, this method is called Six Sigma algorithm. F is the objective function, and M is the target speed of the capsule; hence, the purpose of the optimization is to make the capsule speed be close to the proposed speed step.

3.2 Optimization Case: Forward Movement with Medium Speed

The optimization case for the capsule moving forward with medium speed (5 mm/s) is taken as an example to introduce the whole optimization process. Primarily, all the parameter ranges for the environmental variable and the three optimization parameters are listed in Table 2. In particular, the optimized Latin square method

Table 2 Parameter settings for optimization

Parameters	Unit	Signs	Mode	Lower	Upper
Friction coefficient	–	μ	Input	0.2	0.5
Frequency	Hz	f	Input	1	50.0
Amplitude	N	P_d	Input	0.001	0.03
Duty cycle ratio	%	D	Input	10.0	90.0
Velocity of capsule	mm/s	V_{avg}	Output	0.1	10.0

**Fig. 3** Optimization by integrating Isight and MATLAB. (a) Combination of optimization algorithms; (b) reliability verification of the obtained optimal solution

is applied to build a uniform distribution for the uncertainty friction coefficient, which is an array with 50 different friction coefficients whose values are within 0.2 and 0.5. Furthermore, the lower and upper boundaries for the capsule speed are set as 0.1 mm/s and 10 mm/s, respectively; namely, as a fundamental requirement, the capsule should keep moving forward. Based on the optimization flow built in Isight (see Fig. 3a), in total, 50 combinations of the design parameters were tested, and for each combination, 50 different friction coefficients were simulated; eventually, the average velocity for such combination under the 50 different friction coefficients was calculated. The variations of both the three design parameters and the obtained average velocity of capsule are shown in Fig. 4. From Fig. 4, the average velocity of the capsule cannot be stabilized exactly as 5 mm/s; however, if the design parameters shown in Table 3 are used to excite the capsule system, an approximate speed of 4.5840136 mm/s can be obtained, which can be accepted as the medium speed for the capsule moving forward.

Subsequently, both the variation range of the friction coefficient and the boundaries of the capsule speed are kept to be consistent with that in the optimization process, while the optimization parameters are set to fluctuate slightly near the obtained optimal result; see Table 4. Based on the flow path for the reliability

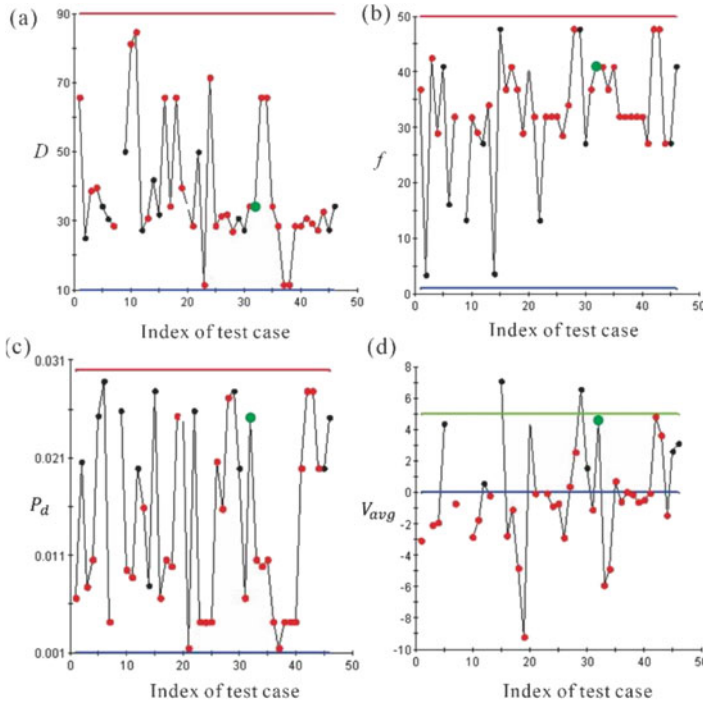


Fig. 4 Variations of the parameters and the capsule speed in the optimization process and the green point in each subplot corresponds to the optimal solution

Table 3 Result of optimization

Parameters	Unit	Values
D	%	34.233768
f	Hz	40.949187
P_d	N	0.0251731
V_{avg}	mm/s	4.5840136

Table 4 Parameter settings for reliability verification

Parameters	Mode	Mean	Lower	Upper	Distribution
μ	Input	0.35	0.2	0.5	Uniform
P_d	Input	0.0251731	0.02473	0.02561	Uniform
f	Input	40.949187	40.2398	41.6584	Uniform
D	Input	34.233768	33.6408	34.8267	Uniform
V_{avg}	Output	4.5840136	0.1	10.0	—

verification shown in Fig. 3b, 1000 combinations of the optimization parameters, whose distributions are shown in Fig. 5, are simulated numerically to check whether the capsule speed crosses the defined boundaries 0.1 mm/s or 10 mm/s. The obtained distribution of the capsule speed is displayed in Fig. 6, and the corresponding

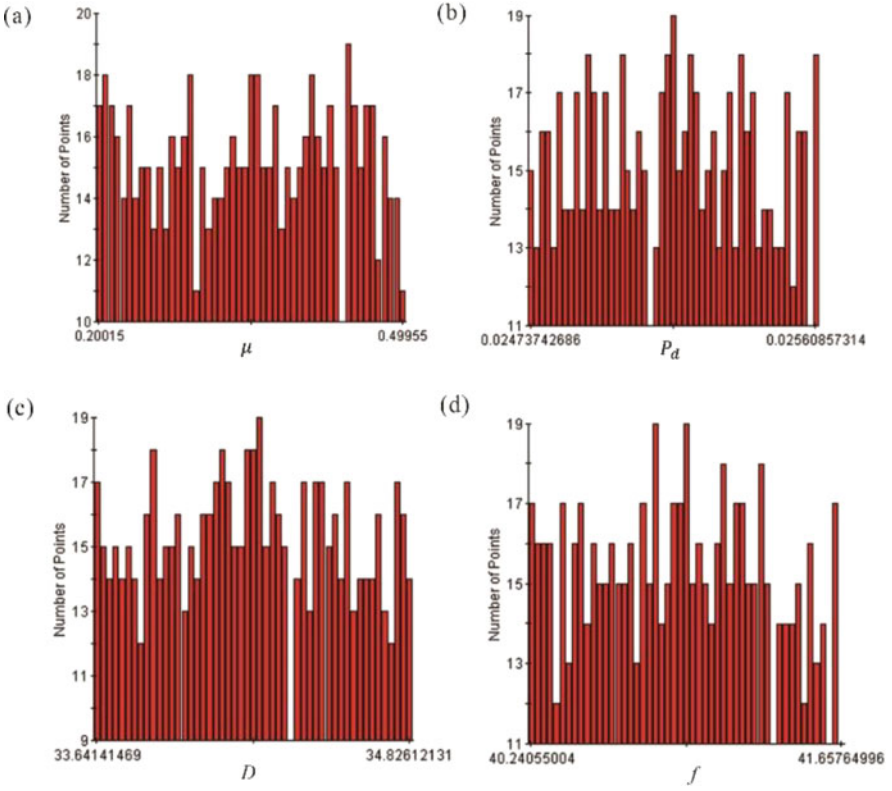


Fig. 5 Distributions of parameters for reliability verification

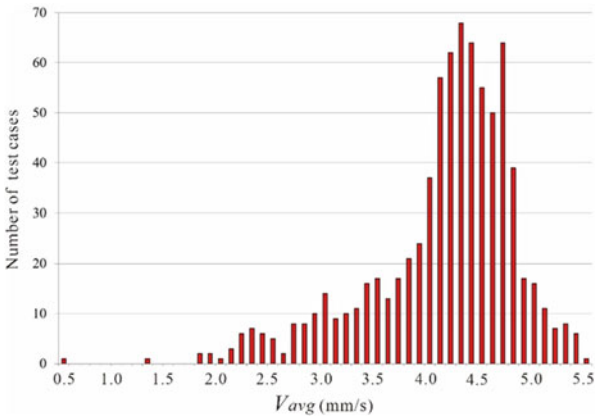


Fig. 6 Distributions of average velocity of capsule for reliability verification

Table 5 Results of reliability verification

Type	Value
Mean velocity	4.091490737
Standard deviation	0.685242201
Minimum velocity	0.505602717
Maximum velocity	5.473377537
Probability between limits	100%

Table 6 Optimization results of seven speed steps for the capsule movement

Speed steps	Target speed (mm/s)	Allowed speed (mm/s)	Optimized parameters			Obtained speed (mm/s)
			f (Hz)	P_d (N)	D (%)	
Fast backward	-10	(-15, -5)	33.77	0.0223	66.86	-9.01
Medium backward	-5	(-10, -0.1)	44.14	0.0242	14.66	-5.05
Slow backward	-1	(-3, -0.1)	44.14	0.0044	25.70	-0.91
Hover	0	(-0.1, 0.1)	21.84	0.0043	86.75	0
Slow forward	1	(0.5, 1.5)	Failed			
Medium forward	5	(0.1, 10)	40.95	0.0251	34.23	4.58
Fast forward	10	(5, 15)	Failed			

statistical result is listed in Table 5, where the reliability for the capsule moving forward is verified as 100%, since, when setting the excitation signal as the obtained optimal combination of parameters, the minimal velocity is around 0.51 mm/s; moreover, the average velocity is 4.1 mm/s which is still close to the predefined medium speed (5 mm/s).

3.3 Optimization Results

By using the same way introduced in Subsection 3.2, the proposed seven speed steps are optimized one by one, and the obtained results are listed in Table 6. Specifically, according to the optimization of excitation parameters for the vibro-impact capsule, five speed steps for the capsule moving steady under uncertain small-bowel environment are explored. However, given the current excitation parameter ranges, the steady slow and fast-forward movements cannot be achieved by the studied capsule. Therefore, if the rest two speed steps are required for the practical application of the capsule system, both the modification of the structure parameters and the broader ranges of control parameters deserve to be tried.

According to the obtained parameter combinations for five different speed steps, the numerical simulations are conducted to observe the changes of the capsule

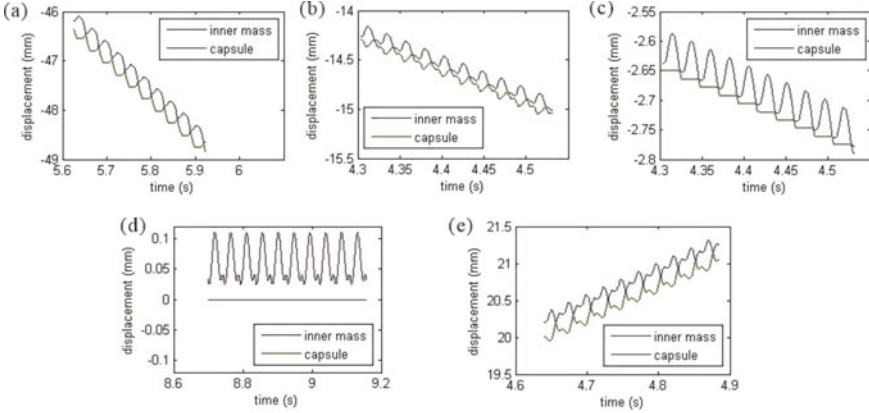


Fig. 7 Results of numerical simulations with different parameter combinations for five different speed steps: (a) fast backward, (b) medium backward, (c) slow backward, (d) hover, and (e) medium forward

speed. For all the five cases, the friction factor is set the same as 0.2293. Eventually, the simulated results are shown in Fig. 7 where the corresponding velocities of the capsule are (a) $v_{\text{avg}} = -8.3068$ mm/s for fast backward, (b) $v_{\text{avg}} = -3.3368$ mm/s for medium backward, (c) $v_{\text{avg}} = -0.6142$ mm/s for slow backward, (d) $v_{\text{avg}} = 0$ mm/s for hover, and (e) $v_{\text{avg}} = 4.28$ mm/s for medium forward. All the obtained five velocities of capsule are close to the predefined targets of speed steps.

4 Concluding Remarks

1. In this paper, a graded variable speed design for a self-propulsion capsule system was carried out, in which three types of movements, including forward, backward, and hover, were considered; meanwhile, the fast, medium, and slow speeds were classified for both the forward and backward movements of the capsule; thus, in total, seven speed steps were defined for the further optimization.
2. According to the seven speed steps defined in this paper, the optimization was conducted via the combination of the MATLAB and Isight software. Specifically, three controllable parameters, including frequency, amplitude, and duty cycle ratio, were optimized, and the influence of the friction coefficient in the uncertain small-bowel environment was also introduced in the optimization process. Finally, it was demonstrated that the capsule can achieve five speed steps: fast backward, medium speed backward, slow backward, hover, and medium speed forward; however, it was also found that for the given structure parameters of the capsule, the stable fast-forward movements and the stable slow forward movements cannot be obtained by the optimization of the three controllable parameters.

3. In future work, by resorting on the guidance of the numerical simulation conducted in this paper, the corresponding variable speed steps will be experimentally tested, and the optimization design method will also be improved according to the obtained experimental results.

References

1. Y. Lee, A. Erdogan, S. Rao, How to assess regional and whole gut transit time with wireless motility capsule. *J. Neuro Gastroenterol. Motil.* **20**(2), 265–270 (2014)
2. F. Carpi, N. Kastelein, M. Talcott, et al., Magnetically controllable gastrointestinal steering of video capsules. *I.E.E.E. Trans. Biomed. Eng.* **58**(2), 231–234 (2011)
3. J. Keller, C. Fibbe, F. Volke, et al., Remote magnetic control of a wireless capsule endoscope in the esophagus is safe and feasible: results of a randomized, clinical trial in healthy volunteers. *Gastrointest. Endosc.* **72**(5), 941–946 (2010)
4. Y. Liu, M. Wiercigroch, E. Pavlovskaja, et al., Modelling of a vibro-impact capsule system. *Int. J. Mech. Sci.* **66**, 2–11 (2013)
5. Y. Liu, E. Pavlovskaja, M. Wiercigroch, Vibro-impact responses of capsule system with various friction models. *Int. J. Mech. Sci.* **72**, 39–54 (2013)
6. Y. Yan, Y. Liu, M. Liao, A comparative study of the vibro-impact capsule systems with one-sided and two-sided constraints. *Nonlinear Dyn.* **89**, 1063–1087 (2017)
7. Y. Liu, E. Pavlovskaja, M. Wiercigroch, Experimental verification of the vibro-impact capsule model. *Nonlinear Dyn.* **83**, 1029–1041 (2013)
8. Y. Yan, Y. Liu, J. Páez Chávez, et al., Proof-of-concept prototype development of the self-propelled capsule system for pipeline inspection. *Meccanica* **53**(8), 1997–2012 (2017)
9. Y. Liu, J. Paez Chavez, J. Zhang, et al., The vibro-impact capsule system in millimetre scale: numerical optimisation and experimental verification. *Meccanica* **55**, 1885–1902 (2020)
10. B. Guo, E. Ley, J. Tian, et al., Experimental and numerical studies of intestinal frictions for propulsive force optimisation of a vibro-impact capsule system. *Nonlinear Dyn.* **101**(1), 65–83 (2020)